THE ASTROPHYSICAL JOURNAL, 497:32–37, 1998 April 10

CLUSTER-GALAXY CORRELATIONS IN COLD DARK MATTER MODELS

MANUEL E. MERCHÁN,[1] MARIO G. ABADI,[2] DIEGO G. LAMBAS,[3] AND CARLOS VALOTTO[1]
Grupo de Investigaciones en Astronomía Teórica y Experimental, Observatorio Astronómico de Córdoba, Laprida 854, 5000, Córdoba, Argentina; manuel@oac.uncor.edu, mario@oac.uncor.edu, dgl@oac.uncor.edu, val@oac.uncor.edu
Received 1997 June 26; accepted 1997 November 18

ABSTRACT

We study the ability of *COBE*-normalized cold dark matter (CDM) models to reproduce observed properties of the distribution of galaxies and clusters using *N*-body numerical simulations. We analyze the galaxy-galaxy and cluster-galaxy two-point correlation functions, ξ_{gg} and ξ_{cg}, in open ($\Omega_0 = 0.4$, $\Omega_\Lambda = 0$, $\sigma_8 = 0.75$) and flat ($\Omega_0 = 0.3$, $\Omega_\Lambda = 0.7$, $\sigma_8 = 1.05$) CDM models, both of which reproduce the observed abundances of rich clusters of galaxies.

To compare models with observations, we compute projected cross-correlation functions ω_{gg} and ω_{cg} to derive the corresponding ξ_{gg} and ξ_{cg}. We use target galaxies selected from the Las Campanas Redshift Survey, target clusters selected from the APM Cluster Survey, and tracer galaxies from the Edinburgh Durham Sky Survey catalog.

We find that the open model is able to reproduce the observed ξ_{gg}, whereas the flat model needs antibias in order to fit the observations. Our estimate of ξ_{cg} for the APM cluster sample analyzed is consistent with a power law $\xi_{cg} = (r/r_0)^\gamma$ with $r_0 = 10.0 \pm 0.7\ h^{-1}$ Mpc and $\gamma \simeq -2.1$. For the open and flat-antibiased CDM models explored we find the corresponding cluster-galaxy correlation lengths $6.5 \pm 0.7\ h^{-1}$ Mpc and $7.2 \pm 0.5\ h^{-1}$ Mpc, respectively, significantly lower than the observed value. Our results indicate that *COBE*-normalized CDM models are not able to reproduce the spatial cross-correlation of clusters and galaxies.

Subject headings: cosmology: observations — cosmology: theory — dark matter — methods: numerical

1. INTRODUCTION

The inflationary scenario and the cold dark matter (CDM) models have become one of the most popular theoretical starting points to describe the formation and evolution of structures in the universe using numerical simulations. Given the failure of the standard CDM model (dimensionless density parameter $\Omega_0 = 1$ and a Hubble constant $H_0 = 100\ h$ km s^{-1} Mpc^{-1} with $h = 0.5$) to reproduce the observed distribution of galaxies at large scales, several attempts have been made in order to construct new consistent models. The introduction of a cosmological constant $[\Omega_\Lambda = \Lambda/(3H_0^2)]$ in the CDM scenario allows for a flat universe ($\Omega = \Omega_0 + \Omega_\Lambda = 1$) with $\Omega_0 < 1$ as suggested by observations. On the other hand, measurements of the *Cosmic Background Explorer* (*COBE*) satellite have determined the normalization of different power spectra of primordial density fluctuations and therefore the present value of the root mean square mass fluctuation σ_8 in spheres of radius 8 h^{-1} Mpc in the models. Recently Cole et al. (1997) analyzed the galaxy-galaxy two-point correlation function in *COBE*-normalized CDM models with different density parameters Ω_0 and cosmological constant Ω_Λ using numerical simulations. The authors explore the ability of these CDM models to reproduce observed cluster number densities. Their results suggest that *COBE*-normalized CDM models with parameters $\Omega_0 = 0.4$, $\Omega_\Lambda = 0$ and $\Omega_0 = 0.3$, $\Omega_\Lambda = 0.7$ (with age of the universe $t_0 \simeq 12$ and 14 Gyr, respectively) provide a suitable fit to observations. These models successfully reproduce observed cluster abundances without requiring a strong bias of the distribution of particles in the simulations in order to fit the observed galaxy-galaxy correlation function.

The two-point correlation functions are powerful statistical tools to compare the observed distribution of galaxies and galaxy clusters and the corresponding model predictions. The autocorrelation function of bright optically selected galaxies is well described by a power-law fit of the form $\xi_{gg}(r) = (r/r_0)^\gamma$ with $\gamma = -1.77$ and $r_0 = 5.4\ h^{-1}$ Mpc (Peebles 1993 and references therein). The joint distribution of galaxies and clusters of galaxies can also be statistically described using the cluster-galaxy two-point cross-correlation function $\xi_{cg}(r)$. Seldner & Peebles (1977) in their cross-correlation analysis of Abell clusters and Lick counts find a suitable power-law fit $\xi_{cg}(r) = (r/r_0)^\gamma$, where $\gamma \simeq -2$ and $r_0 \simeq 15\ h^{-1}$ Mpc. Using similar data, Lilje & Efstathiou (1988) argue for a lower value of amplitude $r_0 \simeq 8.8$ h^{-1} Mpc with slope $\gamma \simeq -2.2$. The reasons for the different reported amplitudes rely mainly on the assumed distribution of redshifts of Lick galaxies and deserve further analysis. Moreover, since several authors have found dependences of the galaxy-galaxy and cluster-galaxy correlation lengths on galaxy luminosity, cluster richness, intracluster gas temperature, and velocity dispersion (Valotto & Lambas 1997; Loveday et al. 1995; Croft et al. 1997; Valotto & Lambas 1995), a careful analysis of the target properties is required to confront models and observations properly.

In this paper we analyze the distribution of galaxies and clusters of galaxies in two *COBE*-normalized CDM models (open and flat) through numerical simulations. We confront the results of the simulations with observations using a sample of clusters of galaxies taken from the APM cluster catalog and a sample of galaxies from the Las Campanas Redshift Survey (Shectman et al. 1996). Section 2 describes the numerical simulations performed, and § 3 deals with the

[1] On a fellowship from the Consejo de Investigaciones Científicas y Tecnológicas de la Provincia de Córdoba (CONICOR), Córdoba, Argentina.

[2] On a fellowship from the Consejo de Investigaciones Científicas y Técnicas de la República Argentina (CONICET), Argentina.

[3] CONICET, Argentina.

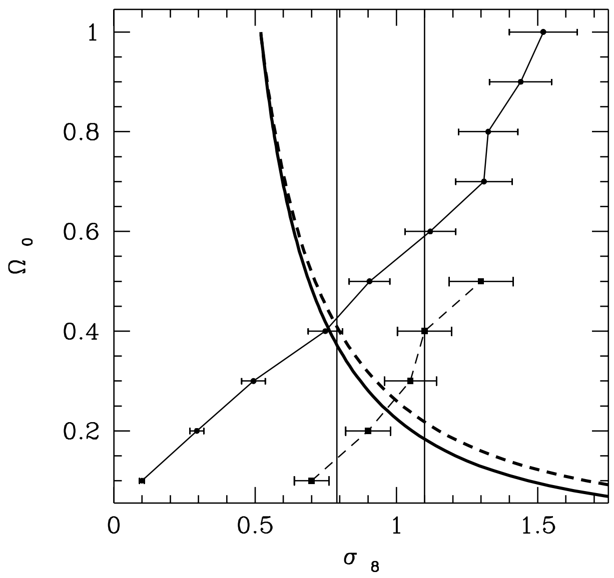

FIG. 1.—Constraints on Ω_0 and σ_8 in CDM models. The thin lines correspond to *COBE* normalization for the open model with $\Omega_\Lambda = 0$ model (*solid line*), and the flat model with $\Omega_\Lambda \neq 0$ (*dashed line*). Similarly, thick lines represent cluster abundances derived by Eke, Cole, & Frenk (1996). The vertical lines correspond to the rms fluctuation in the number of galaxies taking into account the quoted errors in the galaxy-galaxy correlation length (see text). Horizontal error bars for the open model are taken from Table 1 of Gorski et al. (1995) and for the flat model the error bars correspond to 1σ deviations taken from Cole et al. (1997).

analysis of the data. In § 4 we confront model results to observations, and we analyze the ability of the models to reproduce the observed correlation functions.

2. NUMERICAL MODELS

COBE temperature fluctuation measurements allows us to determine the normalization of the CDM mass fluctuation spectrum for different values of Ω_0 and Ω_Λ. In Figure 1 are plotted Ω_0 as a function of σ_8 in *COBE*-normalized

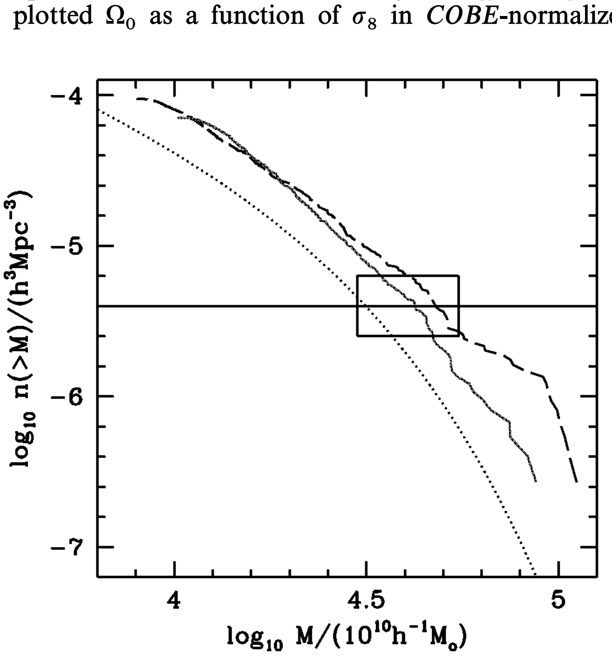

FIG. 2.—Observed cluster abundances given by Bahcall & Cen (1993) (*dotted line*) and the correponding abundances inferred from the open (*solid line*) and flat (*dashed line*) models. The box indicates the observational range of masses with abundance $4 \times 10^{-6}\ h^3$ Mpc^{-3}.

CDM models extracted from Table 1 of Gorski et al. (1995) and from Cole et al. (1997). The solid and dashed thin lines correspond to open models with $\Omega_\Lambda = 0$ and flat models with $\Omega_\Lambda \neq 0$, respectively. In this figure is also shown (*thick line*) the corresponding relation between these parameters found in open CDM models (*dashed line*) and flat (*solid line*) corresponding to the fit of the cluster temperature function computed by Eke, Cole, & Frenk (1996). The intersections of these curves provide the suitable values of the parameters that fit simultaneously cluster abundances and *COBE* normalizations. By inspection of this figure our choice of models that fulfill this condition is apparent: open, with $\Omega = 0.4$, $\Omega_\Lambda = 0$, $\sigma_8 = 0.75$; and flat, with $\Omega = 0.3$, $\Omega_\Lambda = 0.7$, $\sigma_8 = 1.05$ (both with a Hubble parameter $h = 0.65$). The vertical lines show the allowed range of values of σ_8 compatible with the observed relative fluctuations in the number of bright galaxies $\delta N/N = 1.35(r/r_0)^{\gamma/2}$, where $\gamma = -1.77 \pm 0.04$ and $r_0 = 5.4 \pm 1.0\ h^{-1}$ Mpc (Peebles 1993). Thus, no strong biasing of the spatial distribution of particles is required to infer the properties of the galaxy distribution in these models.

For these two models (open and flat) we have performed N-body numerical simulations using the adaptive particle–particle-particle-mesh (AP3M) code developed by Couchman (1991). Initial positions and velocities of particles were generated using the Zeldovich approximation corresponding to the CDM power spectrum. The computational volume is a periodic cube of side length 195 h^{-1} Mpc. We have followed the evolution of $N = 5 \times 10^5$ particles in a 64^3 grid mesh, with four levels of refinements as a maximum. The resulting mass per particle is $4.11 \times 10^{12}\Omega_0$ h^{-1} $M_\odot$. We have adopted an analytic fit to the CDM power spectrum of the form

$$p(k) \propto \frac{k}{[1 + 3.89q + (16.1q)^2 + (5.46q)^3 + (6.71q)^4]^{1/2}} \times \left[\frac{\ln(1 + 2.34q)}{2.34/q}\right]^2 , \quad (1)$$

where $q = (k/\Gamma)\ h$ Mpc $^{-1}$, $\Gamma = \Omega_0\ h \exp[-(\Omega_B + \Omega_B\Omega_0)]$, and $\Omega_B = 0.0125\ h^{-2}$ is the value of the baryon density parameter imposed by nucleosynthesis theory (Bardeen et al. 1986 and Sugiyama 1995). The initial conditions correspond to redshift $z = 10$, and the evolution was followed using 1000 steps.

We identify centers of mass of clumps of particles in the simulations using a standard friends-of-friends algorithm with a linking length $l = 0.17n^{-1/3} = 418\ h^{-1}$ kpc, where n is the mean particle density (Cole et al. 1997). Using these centers, we define the clusters in the simulations as the particles within Abell radius $R_A = 1.5\ h^{-1}$ Mpc and compute the corresponding cluster masses. In Figure 2 we show the resulting cumulative mass function of the two CDM models at redshift $z = 0$ and the analytic fit to observations given by Bahcall & Cen (1993). Following Cole et al. (1997), we show a box indicating the mass range of clusters with observed abundance $4 \times 10^{-6}\ h^3$ Mpc $^{-3}$. As can be appreciated from this figure, there is good agreement between observations and the two models analyzed, consistent with the results of Cole et al. (1997).

3. ANALYSIS OF OBSERVATIONS

In this section we compute the projected two-point cluster-galaxy and galaxy-galaxy cross-correlation function

[$\omega_{cg}(r_p)$ and $\omega_{gg}(r_p)$, respectively], where r_p is the projected distance between targets (clusters or galaxies) and tracers (galaxies). We estimate the projected target-tracer cross-correlation function using

$$\omega(r_p) = \frac{\langle N(r_p) \rangle}{\langle N_{\rm RAN}(r_p) \rangle} - 1 , \qquad (2)$$

where $\langle N(r_p) \rangle$ is the mean number of target-tracer pairs separated by a projected distance r_p in the data and $\langle N_{\rm RAN}(r_p) \rangle$ corresponds to targets with random angular positions and with the same redshift distribution as the data targets.

The determination of the spatial correlation function $\xi(r)$ from $\omega(r_p)$ requires the inversion of

$$w(r_p) = C \int_{-\infty}^{\infty} \xi[(\Delta^2 + r_p^2)^{1/2}] d\Delta . \qquad (3)$$

This integral extends over all line-of-sight separations Δ of target-tracer pairs. The constant C in equation (3) is related to the probability that a tracer galaxy is found at a radial distance d from the observer. Assuming a power-law model for the cross-correlation function $\xi(r) = (r/r_0)^\gamma$, Lilje & Efstathiou (1988) derive

$$w(r_p) = C \sqrt{\pi}\, \frac{\Gamma[-(\gamma+1)/2]}{\Gamma(-\gamma/2)}\, \frac{r_0^{-\gamma}}{r_p^{-(\gamma+1)}} . \qquad (4)$$

Using equation (2), we have computed $\omega(r_p)$, and by fitting power laws, we have inferred correlation lengths r_0 and slopes γ from equation (4).

We have chosen tracer objects corresponding to galaxies in the southern Galactic hemisphere of the Edinburgh-Durham sky survey (hereafter the COSMOS survey). Angular positions and apparent B_j magnitudes are available for all galaxies in COSMOS. At faint magnitudes B_j, misclassification of stars and galaxies, plate zero points, and photometric errors become critical. Taking this fact into account, and in order to check our estimates of the correlation function fitting parameters, we have defined two samples of tracers with limiting B_j magnitudes $m_{\rm lim} = 18.0$ and $m_{\rm lim} = 19.0$. We have selected target clusters from the APM Cluster Survey (Dalton et al. 1994), restricting our analysis to clusters with APM richness $30 < \mathscr{R} < 60$ and with radial velocities in the range 10,000–40,000 km s^{-1}, since the number density of clusters falls rapidly beyond 40,000 km s^{-1}. The lower limit in radial velocity was adopted in order to avoid large angular separations in the computation of correlations. The restriction on APM richness $\mathscr{R}$ is based on the fact that clusters with $\mathscr{R} < 30$ are very poor and their number density continuously falls beyond 15,000 km s^{-1}. There are only eight clusters with $\mathscr{R} > 60$; these objects were also not included in our studies, since their radial velocities are beyond the mean of our sample ($\simeq$25,000 km s^{-1}). It should also be remarked that the selection procedure used to build the APM Cluster Survey makes it free from artificial inhomogeneities (Dalton et al. 1997). We have considered two subsamples according to the richness parameter: $30 < \mathscr{R} < 40$ and $40 < \mathscr{R} < 60$ in order to search for possible richness dependences of cluster-galaxy correlations. To check the consistency of our results, we have also computed ξ_{cg} using samples of clusters taken from David et al. (1993) and Ebeling et al. (1996) that provide intracluster temperatures, and clusters taken from Fadda et al. (1996) that provide estimates of cluster velocity dispersions. From these samples we selected clusters with radial velocities in the same range as that adopted for the APM clusters, and the corresponding analysis serves as an independent reproducibility test of our results.

The sample of target galaxies is taken from the Las Campanas Redshift Survey (hereafter LCRS; Shectman et al. 1996). The average radial velocity of these galaxies is $\simeq$30,000 km s^{-1} and extends to $\simeq$80,000 km s^{-1}. Given uncertainties in the derivation of spatial correlations from projected data, we have attempted to focus our analysis on targets with similar redshift distributions, since real differences of spatial correlations among the samples would be directly reflected in the projected correlation functions. The distribution function of radial velocities of LCRS galaxies is shown by the solid line in Figure 3. For comparison the corresponding distribution of $30 < \mathscr{R} < 60$ APM clusters is also shown (*dashed line*). The dotted line in the figure indicates the resulting distribution of radial velocities of LCRS galaxies, where a radial gradient is imposed through a Monte Carlo rejection algorithm that gives a similar distribution to that of the APM cluster sample (hereafter "restricted LCRS galaxies").

We have adopted power-law fits $\omega(r_p) = A r_p^{(\gamma+1)}$ in the range 0.2 h^{-1} Mpc $< r_p <$ 10 h^{-1} Mpc and 0.2 h^{-1} Mpc $< r_p <$ 4 h^{-1} Mpc for cluster-galaxy and galaxy-galaxy correlations, respectively. In Figure 4 we show $\omega_{gg}(r_p)$ and $\omega_{cg}(r_p)$ and the corresponding power-law least-squares fits. Error bars correspond to estimates derived from the bootstrap resampling technique developed by Barrow, Bhavsar, & Sonoda (1984) with 30 bootstrap target samples. For the derivation of r_0 from equation (4) it is necessary to estimate the constant C as an integral that includes the luminosity function in the case of a magnitude-limited sample of tracers such as the COSMOS catalog. For this purpose, we use a Schechter function fitted to the luminosity function of COSMOS galaxies with parameters $M^* = -19.50 \pm 0.13$, $\alpha = -0.97 \pm 0.15$ (Loveday et al. 1992), a K-correction term of the form $3z$, and a flat cosmology ($\Omega_0 = 1$). It is

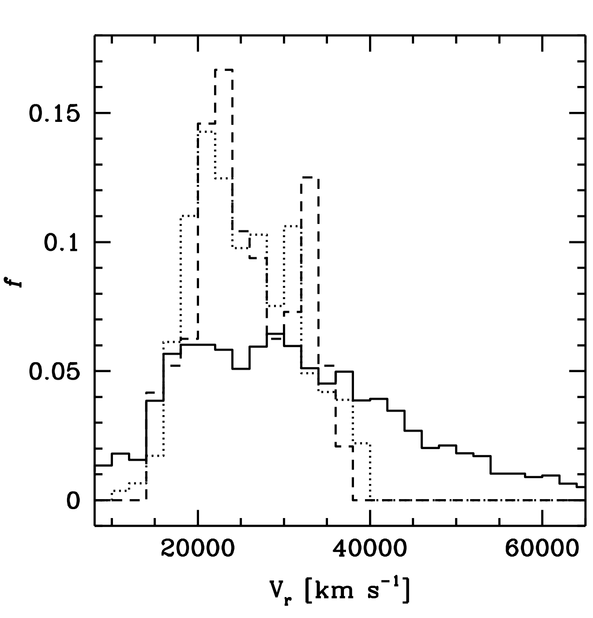

FIG. 3.—Distribution of radial velocities of clusters and galaxies: $30 < \mathscr{R} < 60$ APM clusters (*dashed line*); complete LCRS galaxies (*solid line*); and restricted LCRS galaxies (*dotted line*).

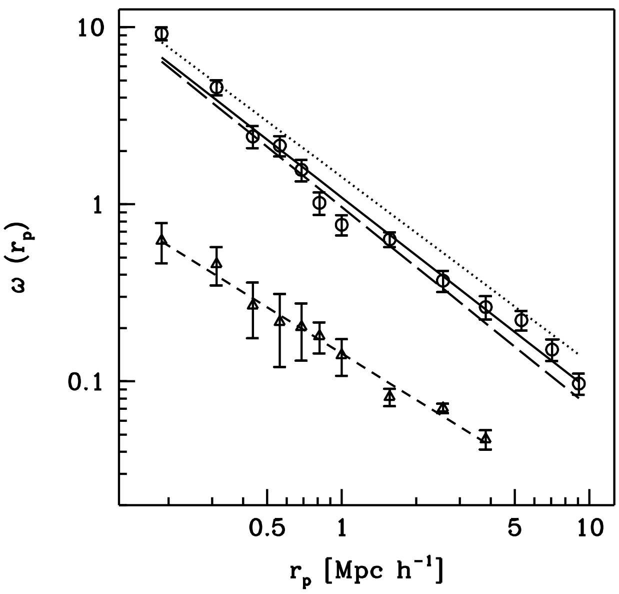

FIG. 4.—Observed projected cross-correlation functions. The circles show $\omega_{cg}(r_p)$ for our sample of 96 APM $30 < \mathscr{R} < 60$ cluster targets and COSMOS survey tracer galaxies with limiting magnitude $m_{lim} = 18$. The solid, long-dashed, and dotted lines correspond to power-law fits of the cluster target samples $30 < \mathscr{R} < 60$, $30 < \mathscr{R} < 40$, and $40 < \mathscr{R} < 60$, respectively. The triangles show $\omega_{gg}(r_p)$ for the restricted LCRS target galaxies and the same COSMOS tracers. The short-dashed line shows the corresponding power-law fit.

important to recall the various sources of error involved in the determinations of the values of r_0 through the inversion of equation (3), such as uncertainties in the luminosity function parameters, K-corrections, and cosmological model, as well as observational biases involving selection effects, photometric errors, etc. The results of our statistical analysis are shown in Table 1. The quoted errors in the values of r_0 were derived through propagation from the rms errors in the ω_{gg} and ω_{cg} power-law fits and variations in C due to uncertainties in the luminosity function parameters, added in quadrature.

From inspection of Table 1, one can notice that the value of the correlation length of the galaxy-galaxy correlation function for the restricted LCRS sample is $r_{0gg} = 3.8 \pm 0.4$ h^{-1} Mpc, lower than the standard value of 5.4 h^{-1} Mpc. This is mostly probably due to a luminosity effect (Loveday et al. 1995; Valotto & Lambas 1997), given that the majority of target galaxies in this sample are $L < L^*$. The values of the cluster-galaxy cross-correlation lengths shown in Table 1 are $\simeq$10%–30% larger than those derived by Lilje & Efstathiou (1988) (except for the $30 < \mathscr{R} < 40$ APM cluster sample), where it can be argued that these differences may rely on the selection function adopted for the Lick catalog. It can also be seen in this table that the richest clusters have larger values of r_{0cg} (Valotto & Lambas 1995). For comparison we have also computed the cross-correlation function for a sample of Abell clusters with measured temperatures and velocity dispersions (Ebeling et al. 1996; Fadda et al. 1996) in the same range of radial velocities. These samples, although with a small number of targets, also show somewhat large values of r_{0cg} compared to the results of Lilje & Efstathiou (1988), consistent with our estimates of APM clusters and giving additional support to our results. It should be remarked that the derived values of the cluster-galaxy correlation length found are not likely to be biased toward high values due to systematics or deprojection calculations, given the relatively low value of the galaxy-galaxy correlation length obtained for targets with an equivalent redshift distribution.

4. COMPARISON BETWEEN MODELS AND OBSERVATIONS

In order to compare the results of observations and numerical models, we have used $30 < \mathscr{R} < 60$ APM clusters, taking advantage of the statistically significant number of target objects in a well-defined volume and the fact that the APM cluster catalog is free from projection and subjective biases. In order to make an appropriate comparison with observations, we have attempted to select a subsample of clusters in the numerical simulations with characteristics comparable to those of this APM cluster sample. Since the APM cluster catalog provides a suitable richness parameter $\mathscr{R}$, we have used 18 APM clusters with measured line-of-sight velocity dispersions σ (Fadda et al. 1996) to provide a suitable relationship between σ and APM cluster richness $\mathscr{R}$. We have also added 15 APM clusters with measured temperatures T (Ebeling et al. 1996) using $\sigma = 400T^{1/2}$, where σ is in kilometers per second and T is in keV. Given the dispersion of the correlation between $\mathscr{R}$ and σ, a simple linear relation of the form $\mathscr{R} = \sigma/19 + 10 \pm 10$ provides a suitable fit to the data. We assign an equivalent APM cluster richness $\mathscr{R}$ to the clusters in the simulations, applying this relation to the actual radial velocity dispersions of the simulated clusters, and select a set of clusters with the same $\mathscr{R}$ distribution and number density (10^{-5} h^3 Mpc^{-3})

TABLE 1

OBSERVATIONAL RESULTS

Sample	N	m_{lim}	C ($\times 10^{-3}$)	A	γ	r_0 (h^{-1} Mpc)
			Galaxies			
LCRS (restricted)	3033	18	3.15	0.16 ± 0.01	-1.91 ± 0.06	3.8 ± 0.4
LCRS (restricted)	3033	19	2.34	0.08 ± 0.01	-1.91 ± 0.04	3.5 ± 0.3
			Clusters			
APM $30 < \mathscr{R} < 60$..............	96	18	3.14	1.09 ± 0.05	-2.09 ± 0.05	10.0 ± 0.7
APM $30 < \mathscr{R} < 60$..............	96	19	2.41	0.96 ± 0.04	-2.04 ± 0.04	10.8 ± 0.6
APM $30 < \mathscr{R} < 40$..............	64	18	3.22	0.97 ± 0.07	-2.13 ± 0.07	8.9 ± 0.8
APM $40 < \mathscr{R} < 60$..............	32	18	2.94	1.42 ± 0.07	-2.05 ± 0.04	12.0 ± 0.8
Fadda et al. 1996 clusters	18	18	3.28	1.09 ± 0.08	-2.00 ± 0.06	10.3 ± 1.0
Ebeling et al. 1996 clusters......	18	18	3.34	1.59 ± 0.08	-2.07 ± 0.04	11.6 ± 0.8

TABLE 2

MODEL RESULTS

Model	γ_{gg}	r_{0gg} (h^{-1} Mpc)	γ_{cg}	r_{0cg} (h^{-1} Mpc)
Open	-2.20 ± 0.08	4.10 ± 0.41	-2.14 ± 0.09	6.54 ± 0.68
Flat	-2.06 ± 0.05	5.90 ± 0.41	-1.88 ± 0.09	8.39 ± 0.83
Flat bias......	-1.90 ± 0.07	4.22 ± 0.39	-1.86 ± 0.06	7.22 ± 0.47

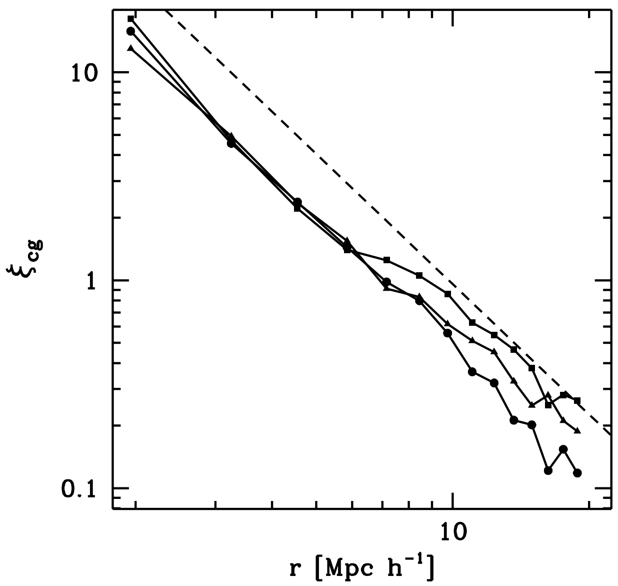

FIG. 5.—Spatial cluster-galaxy cross-correlation function. The dashed line corresponds to the power-law fit $\xi_{cg} = r/(10\ h^{-1}\ \mathrm{Mpc})^{-2.09}$ of the APM cluster sample $30 < \mathscr{R} < 60$. The circles, squares, and triangles correspond to ξ_{cg} of the open, flat, and flat antibiased CDM models, respectively.

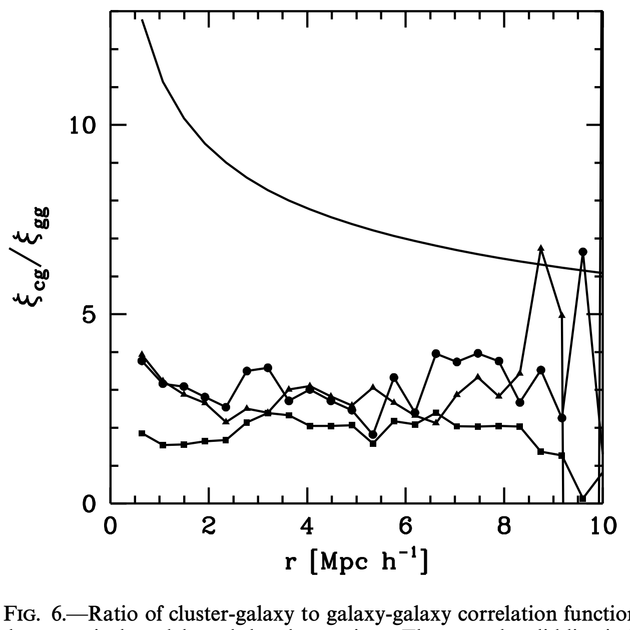

FIG. 6.—Ratio of cluster-galaxy to galaxy-galaxy correlation functions in the numerical models and the observations. The smooth solid line indicates the ratio of the power-law fits (eq. [5]) corresponding to $30 < \mathscr{R} < 60$ APM clusters and the restricted LCRS galaxies ($m_{\lim} = 18$). Circles, squares, and triangles correspond to the open, flat, and flat biased CDM models, respectively.

as those of our $30 < \mathscr{R} < 60$ APM cluster sample. This procedure provides a suitable set of clusters in the numerical simulations that can be confronted with observations.

First, we have considered each particle a galaxy in both open and flat CDM numerical simulations. We have computed the cluster-galaxy, $\xi_{cg}(r) = \langle N_{cg}(r)\rangle/\langle N_{RAN}(r)\rangle - 1$, and galaxy-galaxy, $\xi_{gg}(r) = \langle N_{gg}(r)\rangle/\langle N_{RAN}(r)\rangle - 1$, two-point cross-correlation functions in the numerical simulations where $\langle N_{cg}(r)\rangle$, $\langle N_{gg}(r)\rangle$, and $\langle N_{RAN}(r)\rangle$ are the mean numbers of cluster-galaxy, galaxy-galaxy, and random-galaxy pairs at spatial separation r. The derived cluster-galaxy correlation functions can be fitted by power laws in the range 2 and 20 h^{-1} Mpc. In Table 2 are listed the corresponding values of correlation length r_0 and slope γ of the power-law fits to $\xi_{cg}(r)$ and $\xi_{gg}(r)$ in the models. Quoted uncertainties in this table correspond to errors of the least-squares fits. Errors in r_{0cg} have added in quadrature the corresponding dispersion of values due to the spread in the observed $\mathscr{R}$-σ relation. By comparison of Tables 1 and 2, and in agreement with Cole et al. (1997), it can be seen that the open model requires practically no bias, while the flat model requires a moderate antibias. Because of the failure of the flat model to reproduce the observations, we have generated different mock catalogs of "galaxies" for this model, associating a probability P of the particles being a galaxy according to different prescriptions. We smooth the density field, calculating the density η centered in each particle within a sphere of radius 1.5 h^{-1} Mpc. We have adopted two different models for $P(\eta)$: a power law, $P(\eta) = (\eta/\eta_c)^\alpha$, and a step function, $P(\eta) = 0$ if $\eta > \eta_{\min}$ and $P(\eta) = 1$ otherwise. Both models are constrained to provide a ξ_{gg} consistent with observations. We have found that the cluster-galaxy cross-correlation functions ξ_{cg} of the models for different parameters are very similar. This is expected because the antibias is not too strong and because of the imposed observational constraint on ξ_{gg}. The resulting power-law fitting parameters of $\xi_{gg}(r)$ with $\alpha = 1$ and a suitable value of η_c are shown in Table 2, where the good agreement with observations can be seen for this simple power-law antibiasing model. Nevertheless, the ξ_{cg} of the models do not fit the observations; the cluster-galaxy cross-correlation lengths of the open and flat antibiased CDM models are $\simeq 25\%$ lower than observed, with statistically significant confidence. In Figure 5 are shown the cluster-galaxy correlation function of the models and the observations where the inconsistency of the models is apparent. In order to check the statistical stability of our results, we have taken into account the observed dispersion in the $\mathscr{R}$-σ relation in the selection of clusters in the numerical simulations. We find negligible changes in the correlation lengths of the models, suggesting that our results are not too strongly dependent on the particular selection of the simulated clusters. If only the $\simeq 10$ richest clusters are used in the cross-correlation analysis, significantly larger values of $r_0 \simeq 9\ h^{-1}$ Mpc may be obtained. Certainly this cannot be used for a proper comparison to observations, since the abundance of APM clusters $\gtrsim 1 \times 10^{-5}\ h^3$ Mpc^{-3} corresponds to $\gtrsim 75$ clusters in our computational volume.

The derivation of spatial correlations involves the selection function of COSMOS galaxies and therefore plays an important role in the uncertainties in the luminosity function parameters, K-corrections, etc. The ratio of correlation functions in the power-law approximation is given by

$$\frac{\xi_{cg}(r)}{\xi_{gg}(r)} = \frac{A_{cg} f(\gamma_{gg})}{A_{gg} f(\gamma_{cg})} r^{(\gamma_{cg} - \gamma_{gg})} , \tag{5}$$

where $f(\gamma) = \Gamma[-(\gamma + 1)/2]/\Gamma(-\gamma/2)$, Γ is the gamma function, and A and γ refer to the amplitude and slope of the projected correlation fits, defined in § 3. This ratio is independent of the deprojection uncertainties already mentioned and therefore provides an unbiased measure of the relative clustering of galaxies and galaxy clusters. Figure 6 displays the ratio of the cluster-galaxy to the galaxy-galaxy correlation functions ξ_{cg}/ξ_{gg} for the numerical simulations and the observations. We can see in this figure the large disagreement between the observations and the model results, showing that the observed clusters are in a higher density galaxy environment than the simulated clusters in the CDM models explored.

5. CONCLUSIONS

We have tested an open and a flat Λ-dominated *COBE*-normalized CDM model through the computation of the cluster-galaxy cross-correlation function in order to shed new light on the observational viability of this structure formation scenario. Our analysis of the cluster-galaxy cross-correlation function provides significant statistical evidence of the failure of *COBE*-normalized CDM models to reproduce the extended halos of clusters. In spite of the success of these models in reproducing the abundance of rich clusters and the general pattern of galaxy clustering, the high observed amplitude of cluster-galaxy correlations cannot be reproduced in the models. These results are consistent with the virial analysis of clusters in Cole et al. (1997), where a positive bias is needed in the flat Λ-dominated CDM model to fit observed cluster M/L ratios.

A detailed comparison of models and observations should be stressed, since we have found significant dependences of the cross-correlation function parameters on the velocity dispersion of the clusters in both simulations and observations. Our results rely on a well-controlled sample of galaxy clusters as well as on a comparable set of clusters from numerical simulations, giving confidence in our results as against the ability of *COBE*-normalized CDM models to reproduce the joint distribution of galaxies and clusters.

We thank H. Couchman for kindly providing the AP3M code and Robert Kirshner for kindly permitting the use of the Las Campanas Redshift Survey. This work was partially supported by the Consejo de Investigaciones Cientificas y Tecnicas de la Republica Argentina, the Consejo de Investigaciones Cientificas y Tecnologicas de la Provincia de Cordoba, and the Fundacion Antorchas, Argentina.

REFERENCES

Bahcall, N. A., & Cen, R. 1993, ApJ, 407, L49
Bardeen, J. M., Bond, J. R., Kaiser, N., & Szalay, A. S. 1986, ApJ, 306, 15
Barrow, J. D., Bhavsar, S. P., & Sonoda, D. H. 1984, MNRAS, 210, 19P
Cole, S., Weinberg, D. H., Frenk, C. S., & Ratra, B. 1997, MNRAS, in press
Couchman, H. M. P. 1991, ApJ, 368, L23
Croft, R. A. C., Dalton, G. B., Efstathiou, G., & Sutherland, W. J. 1997, preprint (astro-ph/9701040)
Dalton, G. B., Efstathiou, G., Maddox, S. J., & Sutherland, W. J. 1994, MNRAS, 269, 151
Dalton, G. B., Maddox, S. J., Sutherland, W. J., & Efstathiou, G. 1997, preprint (astro-ph/9701180)
David, L. P., Slyz, A., Jones, C., Forman, W., & Vrtilek, D. 1993, ApJ, 412, 479
Ebeling, H., Voges, W., Bohringer, H., Edge, A. C., Huchra, J. P., & Briel, U. G. 1996, MNRAS, 281, 799
Eke, V. R., Cole, S., & Frenk, C. S. 1996, MNRAS, 282, 263
Fadda, D., Girardi, M., Giuricin, G., Mardirosian, F., & Mezzetti, M. 1996, ApJ, 473, 670
Gorski, K. M., Ratra, B., Sugiyama, N., & Branday A. J. 1995, ApJ, 444, L65
Lilje, P. B., & Efstathiou G. 1988, MNRAS, 231, 635
Loveday, J., Peterson, B. A., Efstathiou, G., & Maddox, S. J. 1992, ApJ, 390, 338
Loveday, J., Maddox, S. J., Efstathiou, G. & Peterson, B. A., 1995, ApJ, 442, 457
Peebles, P. J. E. 1993, Principles of Physical Cosmology (Princeton: Princeton Univ. Press)
Seldner, M., & Peebles, P. J. E. 1977, ApJ, 215, 703
Shectman, S., Landy, S., Oelmer, A., Tucker, D., Lin, H., Kirshner, R., & Schechter, P. 1996, ApJ, 464, 60
Sugiyama, N. 1995, ApJS, 100, 281
Valotto, C. A., & Lambas D. G. 1995, MNRAS, 277, 896
———. 1997, ApJ, 281, 896